Journal of Thermal Analysis and Calorimetry, Vol. 76 (2004) 17–31

INTERACTION OF ACID AND ALKALI TREATED TITANIUM WITH DYNAMIC SIMULATED BODY ENVIRONMENT

J. Strnad[1*], *J. Protivínský*[2], *D. Mazur*[3], *K. Veltruská*[3], *Z. Strnad*[1], *A. Helebrant*[2] *and J. Šesták*[4]

[1]Laboratory for Glass and Ceramics, Lasak Ltd., Papírenská 25, CZ-16000 Prague 6, Czech Republic
[2]Department of Glass and Ceramics, Institute of Chemical Technology, Technická 5, CZ-16628 Praha 6, Czech Republic
[3]Department of Electronics and Vacuum Physics, Faculty of Mathematics and Physics of Charles University, V. Holešovičkách, CZ-18000 Prague 8, Czech Republic
[4]Institute of Physics, Academy of Sciences, Cukrovarnická 10, CZ-16253 Prague 6, Czech Republic

Abstract

Interaction of acid and acid+alkali treated titanium samples with simulated body fluid was studied. In case of alkali treated titanium, the dynamic arrangement of the test enabled the detection of primary calcium and phosphate ion adsorption from the solution and later apatite crystal growth (XRD). The induction time for crystal growth was 24.2 0.3 h. On acid-only treated titanium no crystal growth was detected. The calcium phosphate adsorption layer formed on the acid treated samples was detectable by XPS only, however it differed from that one formed on the acid+alkali treated samples. The adsorption layer formed on the acid+alkali treated samples contained larger amount of calcium, especially in the shortest exposure times. Charging of the apatite crystallites during the XPS measurement enabled the determination their Ca/P ratio separately from Ca/P ratio of the adsorption layers. XPS and EDS analyses indicated that the spherulitic crystallites consisted of carbonated hydroxyapatite with the Ca/P ratio close to that one of the stoichiometric hydroxyapatite. It is proposed that the adsorption layer formed spontaneously and immediately on the acid+alkali treated titanium can provide an ideal interface between the metal implant and the apatite cement line, the first structure formed by osteoblast cells during the formation of the new bone on foreign surfaces.

Keywords: bioactivity, body liquid, calcium phosphate, dental implant, EPS, osseointegration, osteoblast, surface treatment, titanium, XPS

Introduction

Titanium has been the most widely used material for dental implants since the late seventies, when its osseointegrative ability was first discovered and documented [1]. At that time the phenomenon of osseointegration was defined as a formation of an intimate contact of the implant with the bone tissue without intermediate layers on the

* Author for the correspondence: E-mail: strnad@lasak.cz

1388–6150/2004/ $ 20.00

Akadémiai Kiadó, Budapest
Kluwer Academic Publishers, Dordrecht

optical microscopy level. Machined titanium implants were used in the early days; later, implants with surface modifications took over offering more stable and long-term functional interface between the implant and the bone bed. Sand-blasted or titanium plasma sprayed implants showed higher bone-implant contact or removal torque values compared to machined surfaces [2, 3]. Currently, chemical modification of titanium by acid etching is introduced to support and speed-up the healing and the bone formation processes around the implant further [4–8]. The acid etching procedure creates a micro-rough texture that is able to retain the fibrin network of the blood clot, through which cells migrate to the surface of the implant where the new bone is formed [8].

Non-metal bioactive materials such as bioactive glasses, glass-ceramic, silica and titania gels or hydroxyapatite have the ability to form a very stable interface with bone tissue by a formation of a calcium phosphate layer on their surfaces as a consequence of chemical interaction with body fluids [9]. The mechanical strength of this interface usually exceeds the strength of the bone tissue to which bioactive material is bonded [10, 11]. Due to their poor mechanical properties, which disable them from application under load-bearing conditions, bioactive materials (especially hydroxyapatite) are applied onto the surface of titanium implants to achieve faster and more reliable bonding with bone tissue. In spite of the success in accelerating the bone healing process and in the increase of the bone-implant contact in the early phases of healing [12–14], hydroxyapatite plasma sprayed coatings were subject to many controversies regarding their long-term stability.

The ability of bioactive materials to form a bone-like apatite on their surfaces in the body can be reproduced in vitro using a simulated body fluid (SBF) [15]. All bioactive materials, e.g. bioactive glasses, glass-ceramics, SiO_2 and TiO_2 gels, use their hydrated surfaces rich in hydroxyl group to adsorb calcium and phosphate ions and induce spontaneous apatite crystal growth within hours or days [9, 16, 17]. It is the kinetic of precipitation that differs from one material to another [18] and it has been shown that the rate of apatite formation is related to the bone bonding ability of material. The most bioactive of contemporary materials – the 45S5 Bioglass® – forms an interfacial apatite layer 0.8 m thick within 1 h of implantation in a rat bone [19].

In contrast to bioactive materials, machined titanium forms calcium phosphate layers in SBF's at much lower rate and the thickness of the precipitated layers is much smaller. Hanawa [20] used XPS to detect apatite-like calcium phosphate layers after immersing c.p. titanium in Hanks balanced salt solution and after 30 days of soaking the thickness of the adsorbed layer was 7.9 nm. Ducheyne [21] detected a calcium phosphate precipitated on the surface of c.p. titanium by XPS only after 30 days of soaking in SBF. It is assumed that c.p. titanium does not provide such suitable surface for apatite formation as bioactive materials and that this can be the cause of its poorer bone-bonding ability (e.g. compared to hydroxyapatite) especially in shorter healing periods and under non ideal healing conditions [14, 22, 23].

Therefore, various attempts have been made to modify the surface of titanium in order to make it bioactive, but without the use of a thick coating of other bioactive material. The most successful methods of titanium bioactivation are e.g. alkali or fluoride treat-

ment [24]. Especially the ability of alkali-treated titanium to induce apatite precipitation after such short times as 24 h of soaking in SBF was well documented [25, 26].

Surface treatments modifying micro-roughness (acid etching) or bioactivity (alkali etching) showed promising results in tests run in-vivo, as well as superior clinical performance compared to machined or grit blasted surfaces [5–7, 27, 28]. It was found that the combination of treatments, ensuring both optimal roughness and bioactive properties, could result in an implant surface with outstanding ability of quick and reliable osseointegration [29]. It was confirmed that acid+alkali treated titanium surfaces induce reproducible apatite formation in vitro [30] and exhibit promising clinical performance [31].

The ion exchange between the biomaterial's surface and the body fluid is the fastest interaction mode; it precedes and affects the adsorption of larger molecules such as amino acids and proteins. Therefore, a hypothesis can be made that the ion exchange has a profound effect on the later stages of the healing process.

The aim of this study was to compare the initial ion interactions of acid and acid+alkali treated titanium with simulated body fluid (SBF) and to discuss the possible effect of the surface treatments on implant healing.

Materials and methods

Preparation of samples

Titanium samples were used in the form of turnings or titanium discs (diameter 14 mm c.p. Ti grade 4), Fig 1. The machined samples (Ti-M) were washed in isopropanol in an ultrasonic cleaner and dried at 110°C. The first group of samples was acid-etched (Ti-AE) in a solution of hydrochloric acid (40°C, 90 min), washed in deionized (DI) water and ethanol in an ultrasonic cleaner. The second group of samples, designated Ti-AAE in

Fig. 1 Samples - titanium discs and turnings used for exposure in SBF

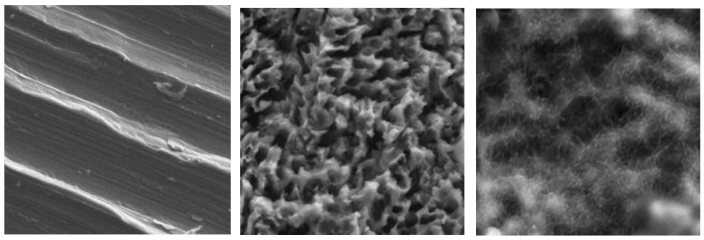

Fig. 2 Surface topography of machined- Ti-M a – acid etched-Ti-AE b – acid and alkali treated – titanium Ti-AAE and c – (SEM, magnification 4000)

this text, was acid-etched under the same conditions and subsequently etched in sodium hydroxide solution (60°C, 4 h), washed in DI water and ethanol in ultrasonic cleaner. All samples were dried at 110°C after washing. The surface topography is showed in Fig. 2.

Experimental arrangement

The SBF solution was prepared using following reagents: KCl, NaCl, $NaHCO_3$, $MgSO_4$ $7H_2O$, $CaCl_2$, Tris, NaN_3 and KH_2PO_4. Tris buffer was used to adjust the pH to 7.55–7.60 at 25°C. Sodium azide was added to inhibit bacterial growth. Samples were exposed in a flow-through reaction cell with SBF preheated at 37°C (Fig. 3). The flow rate of SBF solution through the cell was 0.042 mL min^{-1}. Samples of the output solution were collected for calcium and phosphate ion concentration measurement (Fig. 4). The composition of SBF in comparison to the inorganic part of the blood plasma is given in Table 1. The preparation of the solution was carried out after Jonasova *et al*. [32].

The exposure in SBF is usually carried out as a static experiment, where a sample is placed in the SBF solution of a constant volume, or the solution is periodically renewed [14, 21, 33]. If the solution volume is sufficiently high to keep approximately constant solution composition it is difficult to detect compositional changes in the solution caused by the material-SBF interaction. If the volume is small, concentration changes are measurable but in case of apatite formation the driving force for nucleation and crystallization decreases as calcium and phosphate ions are consumed from the solution. Static exposure

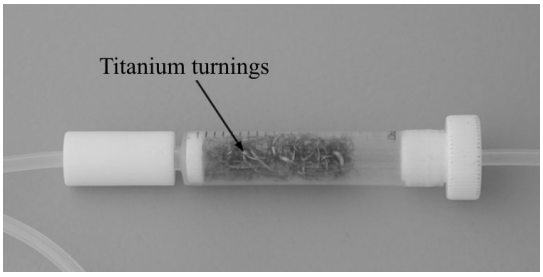

Fig. 3 Flow-through cell used for exposure of samples to SBF

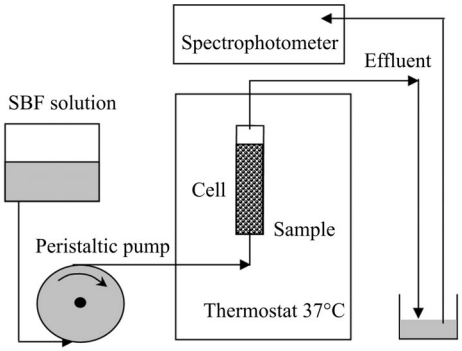

Fig. 4 Experimental arrangement of the exposure in SBF

Table 1 The composition of SBF used in experiments compared to that of human blood plasma

	SBF/mmol L^{-1}	Blood plasma/mmol L^{-1}
Na^+	142.0	137–147.0
K^+	5.0	3.8–5.1
Ca^{2+}	2.5	2.25–2.75
Mg^{2+}	1.0	0.75–1.25
Cl^-	131.0	98–106
HCO_3^-	5.0	24–35
HPO_4^{2-}	1.0	0.65–1.62
SO_4^{2-}	0.5	0.5

also does not resemble the conditions during implantation, where blood circulates. Therefore, a dynamic exposure is suggested to keep constant composition during the experiment and to detect compositional changes in SBF during the initial stages of interaction.

Surface and solution analysis

Composition of the Ti samples' surfaces was analyzed using X-ray photoelectron spectroscopy. UHV facility with Microtech X-ray source and Omicron multi-channel hemispherical analyzer EA 125 was used. The source has Mg/Al dual anode and the Mg anode was used for the measurements. The X-rays were not monochromated. The photoelectron spectra were measured with the analyzer pass energy of 20 eV. The spectra were fitted using a standard fitting procedure with Gaussian–Lorentzian curves.

After exposure in SBF the surface of samples was analyzed by Scanning electron microscopy and energy dispersive spectroscopy (SEM-EDS, Jeol XA-733-superprobe, Jeol USA, Inc.). The EDS analysis results are based on semi-quantitative analysis without the use of standards. X-ray diffraction (XRD) measurements were performed using 3000P diffractometer, Cu anode, measured at 40 kV, 30 mA (Seifert Co., Ahrensburg, Germany).

The concentration of calcium in the output solution was determined using atomic absorption spectroscopy (Varian-Spectr AA300) and phosphate concentration was determined spectrophotometrically (UV-1201, Shimadzu Europe, Ltd.).

The rate of hydration of the prepared titanium samples was measured using FTIR (Fourier transformed infra-red) spectroscopy (Nicolet 740, Nicolet Madison, USA). A wavenumber interval of 400–4000 cm^{-1} was used. Incident radiation angle was 45°.

Results and discussion

Concentration changes in the output solution

The time dependence of Ca^{2+} and PO_4^{3-} ion concentration in the output solution, measured after exposure of Ti-AAE samples in SBF, indicated three main phases of interaction (Fig. 5). First, a rapid but temporary decrease of calcium and phosphate

concentration in the effluent was detected. This decrease indicated a significant adsorption of Ca^{2+} and PO_4^{3-} ions by the material. During the second phase, effluent concentration almost returned to its initial value (100 mg L^{-1} Ca^{2+}, 96 mg L^{-1} PO_4^{3-}). Approximately 25 h from the beginning of the experiment, another concentration decrease was detected. This concentration decrease stabilized at the level of 60–63 mg L^{-1} of PO_4^{3-}, indicating the crystal growth at a constant rate. The formation of apatite crystals on the surface of Ti-AAE samples was also confirmed by SEM and XRD measurement (Figs 8, 11).

The dynamic experimental arrangement enabled simple determination of the induction times using a plot of total mass of PO_4^{3-} consumed by samples' surfaces *vs*. time and by extrapolation of its late-time linear part to the zero mass (Fig. 6). After the induction period, a spontaneous consumption of calcium and phosphate ions from the solution occurred. The induction time value, which is 24.2 0.3 h, is in good agreement with the results obtained using static exposure and reported earlier [26, 34]. In case of Ti-AAE samples the initial calcium and phosphate adsorption was remarkable in the time dependence of the output ion concentrations. The amount of calcium and phosphate ions adsorbed was significantly higher than in case of Ti-AE samples, where no changes in the effluent concentration were detected (Fig. 5).

The finding that only Ti-AAE samples induce apatite formation is in agreement with results of Nancollas *et al*. [35], who detected apatite growth only on the KOH treated titanium surface, whereas on acid (HNO_3) treated titanium the growth did not occur within 3 days of exposure.

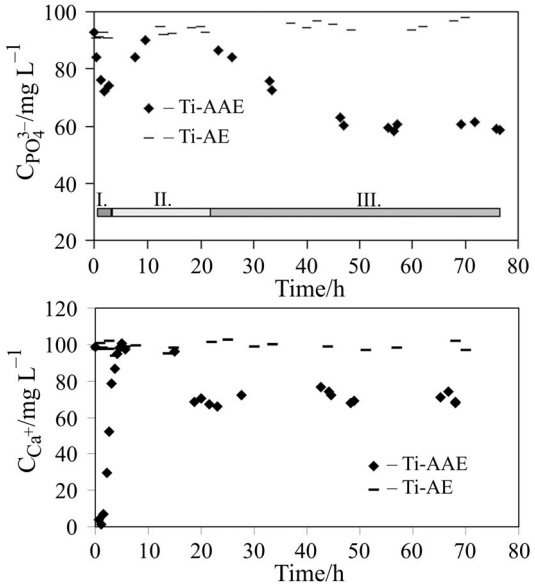

Fig. 5 Time dependence of the PO_4^{3-} and Ca^{2+} concentration in the output SBF solution during exposure of Ti-AE (upper) and Ti-AAE (below) samples, indicating three phases of interaction

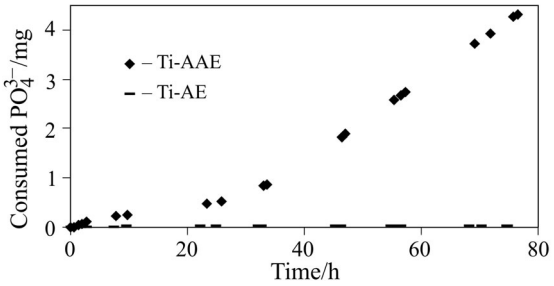

Fig. 6 Time dependence of the precipitated PO_4^{3-} mass plotted for Ti-AAE and Ti-AE samples

FTIR analysis

It was found by Li [16] that not only the negative charge of hydroxyl groups (of titanium oxides) but also their high density on the surface is necessary prerequisite for apatite formation. The FTIR analysis was used to determine the level of hydration of the titanium samples. The peak intensity of hydroxyl groups in the wavenumber range of 3300–3600 was evaluated. The Ti-AAE samples showed significantly higher absorption at 3384.50 cm^{-1} (1.36 Kubelka–Munk units, Fig. 7) compared to Ti-AE samples. The absorption of the Ti-M samples was negligible compared to Ti-AAE. The position of the peak is characteristic to OH groups present e.g. in sol–gel prepared TiO_2 films [36].

These results indicate that the ability of alkali-treated titanium to induce apatite formation can be caused by higher density of hydroxyl groups present in its porous gel-like structure compared to the lower density on the acid-treatedtitanium.

The results of the dynamic flow-through test (Fig. 5) and XPS analysis (Fig. 9) indicate that although ion adsorption occurs on both acid and alkali treated titanium

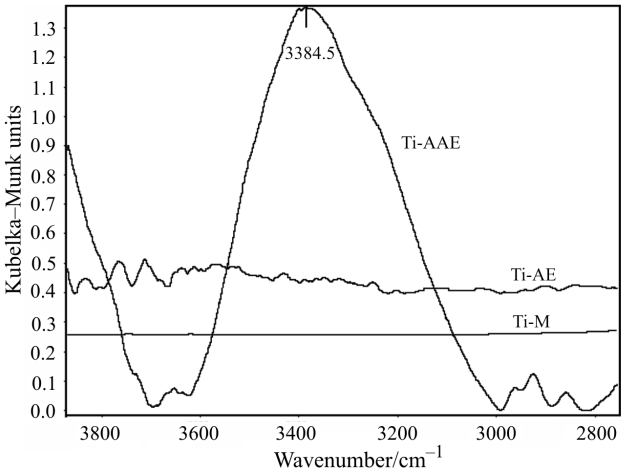

Fig. 7 The FTIR spectrum of Ti-M, Ti-AE and Ti-AAE samples

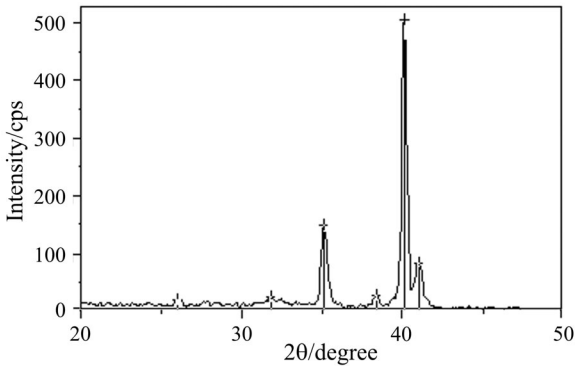

Fig. 8 XRD spectrum of the Ti-AAE sample after 48 h of exposure in SBF solution

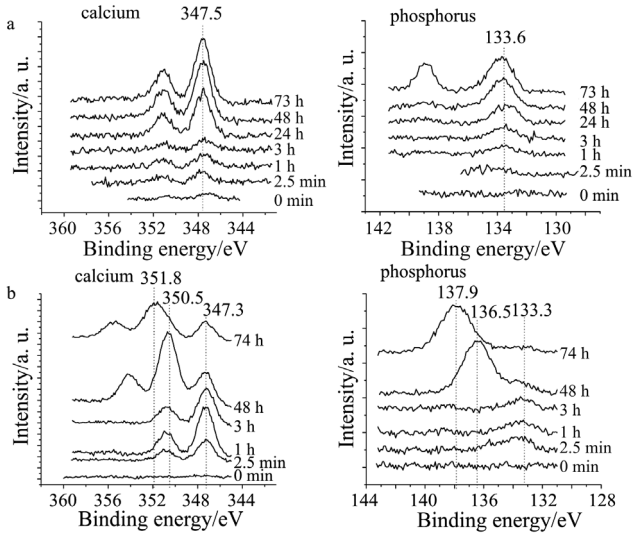

Fig. 9 Photoelectron spectra of Ca 2p and P 2p of a – Ti-AE (HCl-corroded) samples b – Ti-AAE (HCl+NaOH-treated) samples and c – immersed in SBF for various periods of time

surfaces, the adsorbed amount of phosphate and especially calcium ions is larger in case of more hydrated alkali-treated titanium in the first stages of interaction. This could be caused by the detected difference in the density of hydroxyl groups present on the surface of Ti-AAE and Ti-AE samples. It was shown that during the process of peri-implant healing, calcium phosphate cement line containing non-collagenous proteins is formed on the implant's surface before collagenous matrix formation occurs [37, 38].

Intensive calcium adsorption mediated by hydroxyl groups can induce apatite crystal growth but also attract non-collagenous proteins as good calcium binders [39]. By this mechanism an apatite-protein cement layer can be formed on the surface of an implant. Chemical and structural similarity between the preformed cement layer on the

implant's surface and that one produced later by cells can result in a faster formation of a more mechanically stable interface with newly formed bone tissue.

XRD analysis

Although apatite crystallites did not cover the surface of Ti-AAE samples completely, it was possible to detect weak diffraction peaks confirming the presence of hydroxyapatite crystalline phase (Fig. 8).

XPS analysis

On the sample Ti-AE (corroded in HCl without subsequent SBF treatment) carbon C, nitrogen N, oxygen O and titanium Ti were detected, sodium Na was present in barely detectable amount. In the spectrum of Ti-AAE sample (before SBF treatment) sodium Na 1s signal was more intense (by ~3 orders of magnitude) than for Ti-AE sample, as a result of the NaOH treatment. The energetic intervals measured in the photoelectron spectra were those of C 1s, N 1s, O 1s, Na 1s, Ti 2p, Ca 2p and P 2p. In this work, the evolution of calcium and phosphorus spectra was crucial and it will be discussed in detail.

The spectra of carbon, oxygen, calcium and phosphorus exhibited substantially different behavior in case of Ti-AAE compared to Ti-AE samples. In this article, the Ca 2p and P 2p spectra (Fig. 9) are used for illustration. Spectra of O 1s and C 1s evolved likely and they are not shown here. The spectra of Ti 2p showed no difference (between Ti-AE and Ti-AAE samples) and no evolution in peak positions, as well as the N 1s spectra. The intensity of Na 1s peak in Ti-AAE measurements decreased with time in SBF in agreement with models of Kim *et al*. [40] and de Andrade *et al*. [41], for Ti-AE it remained at the just detectable intensity mentioned above. All the analyzed spectra, including those in Fig. 9, were corrected with respect to position of C 1s peak at 285.0 eV to eliminate the shifts in peak positions due to surface charging under X-ray illumination. As shown in Fig. 9, the calcium peak position in case of Ti-AE samples is 347.5 eV, whereas in case of Ti-AAE samples it is 347.3 eV. Additionally, the spectra of Ca 2p of Ti-AAE samples divide in two overlapping peak doublets for the 48 and 74 h periods of SBF treatment. The non-shifted Ca 2p position at 347.3 eV (Ti-AAE samples) corresponds to that of hydroxyapatite [42].

Phosphorus spectra exhibit a similar behavior. For Ti-AE samples, the P 2p peak position is 133.6 eV and it does not change with time of SBF treatment (peak at 138.7 eV shall be discussed later). In case of Ti-AAE samples, the P 2p peak is at 133.3 eV with additional peaks at 136.5 and 137.9 eV, appearing at 48 and 74 h in SBF, respectively. The non-shifted P 2p position at 133.3 eV (Ti-AAE samples) corresponds to that of hydroxyapatite [43].

As shown in Fig. 9, additional intense peaks appeared in calcium and phosphorus spectra of Ti-AAE samples treated in SBF for 48 and 74 h periods. These new peaks are shifted by 3.2 and 4.5 eV, respectively. Similar new peaks at the same shifts from basic positions were observed in the C 1s and O 1s spectra (not shown here),

too. In coherence with SEM observation of crystal growth on the Ti-AAE samples (48 and 74 h of SBF treatment, see SEM-EDS results below) we conclude that the shifted signal comes from the crystallites. The constitution of calcium, phosphorus, oxygen and carbon indicates a carbonated calcium-phosphate nature of the crystallites. Being of insulating nature, the crystallites take on electrical charge. Since they charged independently from the sample surface, i.e. much more, it was possible to distinguish them from the adsorbed calcium- and phosphate-rich layer. The large shift may also indicate their weak bond to the sample surface. The peak at 138.7 eV in P 2p (74 h of SBF treatment) spectrum stands out of all other data, because no spectrum of other elements has shown such a feature. Having eliminated the possibility of presence of foreign element as an impurity on the sample, it was suggested that some phosphorus-based clusters may have formed on the surface. However, another experiment will have to be done to verify this suggestion.

The Ca/P ratios measured for Ti-AE samples and Ti-AAE samples are shown in Fig. 10. Supposing that all 'charged' signal comes from HA crystallites, the Ca/P ratios for the crystallites and for the adsorbed calcium phosphate were calculated separately. For the Ti-AAE samples the Ca/P ratio of the adsorbed layer varies from 2.5 up to 6.2. The Ca/P ratio of the crystallites is in the range from 1.0 to 1.7, that is, significantly lower than the Ca/P ratio of the adsorbed layer. This relation between Ca/P ratios of the adsorbed layer and the growing crystallites corresponds to the model of Takadama *et al*. [43] saying that the calcium deposition precedes the deposition of phosphate groups. The values of Ca/P ratio for the set of Ti-AE samples were between 0.7 and 1.4, which is lower than any of the previous.

From the calcium and phosphorus photoelectron peak positions, as well as from the Ca/P ratio measurements, it can be concluded, that crystallites appearing at Ti-AAE (HCl+NaOH-treated) surfaces consist of carbonated hydroxyapatite. The adsorbed precursor layer created on the surface within the first 24 h could be distinguished from the hydroxyapatite crystallites on basis of the Ca/P ratio, under the as-

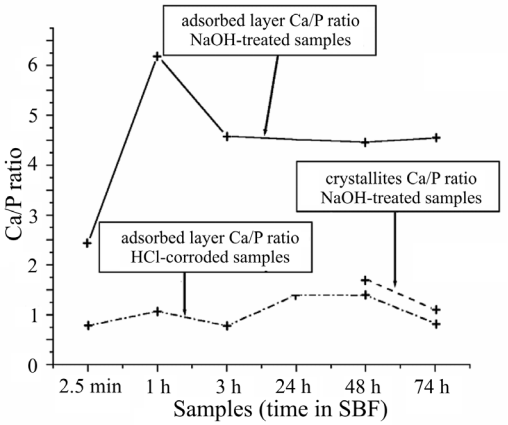

Fig. 10 The Ca/P ratios measured for the Ti-AE (HCl-corroded) samples and Ti-AAE (HCl+NaOH-treated) samples, immersed in SBF for various periods of time

sumption of crystallites charging independently on the adsorbed precursor layer. Between these two no significant difference in binding energies of elements involved has been observed. On the samples with sole HCl treatment (Ti-AE samples), a thin layer of a calcium phosphate (not detected by other methods used), which differs from HA, is created. The Ca/P ratio here is remarkably lower than the Ca/P ratio of the layer adsorbed on NaOH treated (Ti-AAE) samples and the binding energies peak positions differ from those of HA, as discussed above. The primary calcium- and phosphate-rich layers adsorbed on surfaces of Ti-AE and Ti-AAE samples could not be assigned more specific chemical formulae at a reasonable level of confidence. It is a consequence of complicated surface morphology, as well as the fact that XPS spectra of several representatives from the calcium-phosphates family differ too little to distinguish in our measurements [42]. The atomic Ca/P ratio of the crystallites, the coherence in shifts in Ca 2p, P 2p, C 1s and O 1s spectra (48 and 74 h in SBF), and the Ca 2p and P 2p peak positions lead us to a conclusion that the calcium-phosphate developed to the crystals on the Ti-AAE surfaces is most likely carbonated hydroxyapatite. From the Ca/P ratios and SEM observation we conclude that the higher relative abundance of calcium atoms in the adsorbed precursor layer is essential for later formation of hydroxyapatite crystallites.

SEM-EDS

SEM-EDS method was used to detect the changes in the surface structure during exposure in SBF and to analyze precipitates formed on the surface of samples. Figure 11 shows the porous structure of the Ti-AAE samples after exposure in SBF. It can be seen that after 2.5 min up to 24 h only small denser (lighter) areas are formed. These can represent possible nucleation sites of future apatite crystal

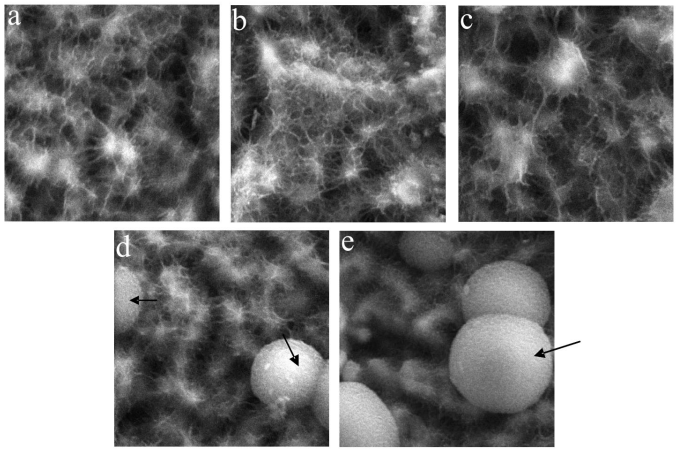

Fig. 11 The surface structure of the Ti-AAE samples after exposure in SBF for a – 2.5 min and b – 1 h c – 24 h d – 48 h e – 72 h (SEM, mag. 4000) (arrows mark the apatite crystallites)

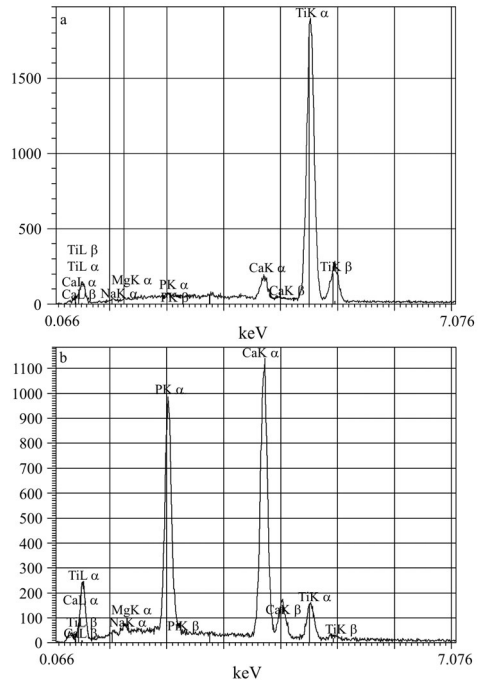

Fig. 12 EDS analysis of the a – crystallite b – the substrate of the sample not covered by the crystallites after exposure of Ti-AAE sample in SBF for 48 h

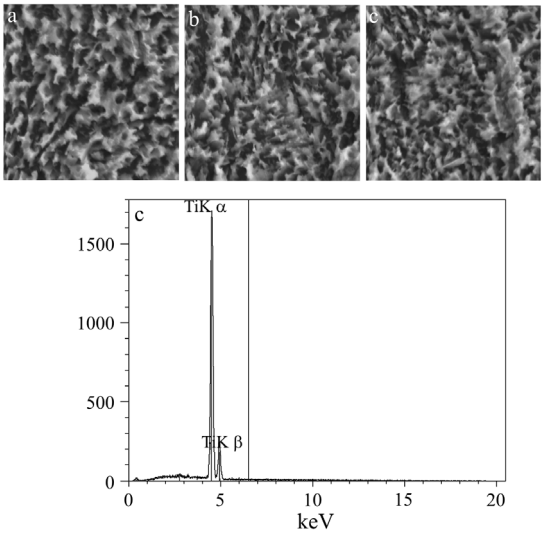

Fig. 13 Surface of the Ti-AE samples after a – 24, b – 48 and c – 72 h of soaking in SBF together with EDS analysis (below) after 48 h of soaking in SBF (SEM-EDS, magnification 4000)

growth. On the sample exposed in SBF for 48 and 72 h formation of crystallites was observed. The SEM-EDS analysis of the Ti-AAE sample exposed in SBF for 48 h is shown in Fig. 12. The analysis indicates that the surface of Ti-AAE sample (not covered by the precipitating crystallites) after exposure in SBF contains a detectable amount of calcium but not detectable (by EDS) amount of phosphorus. The EDS analysis from the spherical crystallite (Fig. 12b) shows strong lines of calcium and phosphorus in the atomic ratio of 1.77, which is slightly higher than that one of stoichiometric hydroxyapatite (1.67). From EDS and XPS results we conclude that spherical bodies consist of hydroxyapatite.

The Ti-AE samples did not show any difference in surface structure and EDS analysis during the exposure in SBF and only titanium was detected after 48 h in SBF (Fig. 13).

Conclusions

The solution analysis during the dynamic SBF test detected calcium and phosphate ionadsorption on the acid+alkali-etched samples in the first stages of interaction. This method was not sensitive enough to detect less intense adsorption in case of Ti-AE samples, where the adsorption layer was detected by XPS analysis. Already after the shortest exposure time of 2.5 min the adsorption layer on the acid+alkali treated samples contained larger amounts of phosphate and especially calcium (also Ca/P ratio was significantly higher than in the case of acid-treated samples). After the induction time of 24.2 h the acid+alkali treated titanium induced apatite crystal growth. The onset of the crystal growth was clearly indicated by the solution analysis.

Charging of the spherulitic crystallites during the XPS measurements allowed us to determine the Ca/P ratio separately for the adsorption layer and the crystallites. Using XPS and EDS analysis the crystallites were identified as carbonated apatite with the Ca/P ratio close to that of stoichiometric apatite. The determination of the induction time could serve as a measure of a substrate ability to support apatite nucleation and growth. The alkali-treated titanium compared to the acid-treated one induced apatite formation in vitro and could therefore provide a suitable substrate for apatite like calcium phosphate precipitates in the cement lines formed on the implants surfaces during the process of new bone formation.

The study is continuation of the series of our communication dealing with glass-ceramic substance and surfaces [44, 45] perspective as mimetic materials for the bone tissue substitution particularly applicable in the dental practice.

This study was supported by the Ministry of Industry and Trade of Czech Republic under the project number FB-CV/64 as well as by the Grant Agency of Academy of Sciences of Czech Republic under the project number A 4010101 and was also a part of the research program MŠMT 113200002 financed by the Ministry of Education of Czech Republic.

References

1 P. I. Brånemark, Scand. J. Plast. Reconstr. Surg., 3 (1969) 81.
2 A. Wennerberg, T. Albrektsson, C. Johansson and B. Andersson, Biomaterials, 17 (1996) 15.
3 K. Gotfredsen, T. Berglundh and J. Lindhe, Clin. Implant. Dent. Relat. Res., 2 (2000) 120.
4 M. Roccuzzo, M. Bunino, F. Prioglio and S. D. Bianchi, Clin. Oral Implants Res., 12 (2001) 572.
5 D. L. Cochran, D. Buser, C. M. Bruggenkate, D. Weingart, T. M. Taylor, J. P. Bernard, F. Peters and J. P. Simpson, Clin. Oral Implants Res., 13 (2002) 144.
6 P. R. Klokkevold, P. Johnson, S. Dadgostari, A. Caputo, J. E. Davies and R. D. Nishimura, Clin. Oral Implants Res., 12 (2001) 350.
7 W. Khang, S. Feldman, C. E. Hawley and J. Gunsolley, J. Periodontol, 72 (2001) 1384.
8 R. J. Lazzara, Bone response to Dual Acid-Etched and Machined Titanium Implant Surfaces. In: J. E. Davies (Ed.) 'Bone engineering' Toronto, Em squared Inc 2000, p. 381.
9 T. Yamamuro, L. L. Hench and J. Wilson, Handbook of Bioactive Ceramics, CRC Press 1990.
10 T. Kokubo, S. Ito, M. Shigematsu, S. Sakka and T. Yamamuro, J. Mater. Sci., 22 (1987) 4067.
11 U. Gross, R. Kinne, H. J. Schmitz and V. Strunz, CRC Critical Reviews in Biocompatibility, 4 (1988) 2.
12 S. Vercaigne, J. G. Wolke, I. Naert and J. A. Jansen, Oral. Implants Res., 9 (1998) 261.
13 L. Sun, C. C. Berndt, K. A. Gross and A. Kucuk, J. Biomed. Mater. Res., 58 (2001) 570.
14 Z. Strnad, J. Strnad, C. Povýšil and K. Urban, J. Oral and Maxillofacial Implants, 15 (2000) 483.
15 T. Kokubo, H. Kushitani, S. Sakka, T. Kitsugi and T. Yamamuro, Mater. Res., 24 (1990) 721.
16 P. Li, C. Ohtsuki, T. Kokubo, K. Nakanishi, N. Soga and K. de Groot, J. Biomed. Mater. Res., 28 (1994) 7.
17 P. Li, X. Ye, I. Kangasniemi, J. M. de Blieck-Hogervorst, C. P. Klein and K. de Groot, J. Biomed. Mater. Res., 29 (1995) 325.
18 L. L. Hench, Surface reaction Kinetics and Adsorption of biological moieties: A mechanistic Approach to tissue Attachment. In J. E. Davies (Ed.), Bone engineering, Toronto, Em. squared Inc. 2000, p. 381.
19 L. L. Hench and O. Andersson, Bioactive glasses. In: L. L. Hench, J. Wilson (Eds) 'An introduction to bioceramics', Florida, World Scientific Publishing 1993, p. 41.
20 T. Hanawa, Titanium and its oxide film: A substrate for formation of apatite. In: J. E. Davies (Ed.) Bone-biomaterial interface, Toronto, Em squared Inc. 2000, p. 49.
21 P. Li and P. Ducheyne, J. Biomed. Mater. Res., 41 (1998) 341.
22 K. Soballe, Acta Orthop. Scand. Suppl., 255 (1993) 1.
23 K. Soballe, E. S. Hansen, H. Brockstedt-Rasmussen, V. E. Hjortdal, G. I. Juhl, C. M. Pedersen, I. Hvid and C. Bunger, Clin. Orthop., 272 (1991) 300.
24 J. E. Elingsen, On the properties of surface-modified titanium. In: J. E. Davies, (Ed.) Bone engineering, Toronto, Em squared Inc. 2000, p. 183.
25 H. M. Kim, F. Miyaji and T. Kokubo, J. Mater. Sci.: Mater. in Medicine, 8 (1997) 341.
26 H. M. Kim, F. Miyaji, T. Kokubo, S. Nishiguchi and T. Nakamura, J. Biomed. Mater. Res., 45 (1999) 100.
27 T. Kokubo, H. M. Kim, S. Nishiguchi and T. Nakamura, In vivo formation induced on titanium metal and its alloys by chemical treatment in Bioceramics. In: Proceedings of the 13 th Int. Symp. on Ceramics in Medicine, Bologna, Italy, Trans. Tech. 2001, p. 3.

28 S. Nishiguchi, T. Nakamura, M. Kobayashi, W. O. Yan, H. M. Kim, F. Miyaji and T. Kokubo, The effect of heat treatment on bone bonding ability of alkali-treated titanium. In: Bioceramics, Vol. 10, Proceedings of the 10th Int. Symp. on Ceramics in Medicine, Paris, France, Elsevier 1997, p. 561.
29 A. Šimůnek, J. Strnad, J. Novák, Z. Strnad, D. Kopecká and R. Mounajjed, Clin. Oral. Impl. Res., 12 (2001) 393.
30 L. Jonášová and J. Hlaváč, Effect of chemical treatment of titanium on apatite formation. In: H. Stallforth and P. Revell (Eds) 'Materials for medical engineering', Euromat 99, Weinheim, Wiley-VCH 2000, p. 126.
31 A. Šimůnek, J. Strnad and A. Štěpánek, Clin. Oral Impl. Res., 13 (2002) 4.
32 A. Helebrant, L. Jonášová and L. Šanda, Ceramics/Silikáty (Prague), 46 (2002) 9.
33 K. Hata, T. Kokubo, T. Nakamura and T. Yamamuro, J. Am. Ceram. Soc., 78 (1995) 1049.
34 J. Strnad, A. Helebrant and J. Hamáčková, Glastech. Ber. Glass. Sci. Technol., 73 (2000) C1.
35 G. H. Nancollas and W. Wu, The controlled nucleation and growth of selected calcium phosphate phases on modified titanium implant surfaces. In: Proceedings of Sixth World Biomaterial Congress, Hawaii: Society for Biomaterials, USA 2000.
36 Y. Djaoued, S. Badilescu, P. V. Ashrit and J. Robichaud, Internat. J. Vibrational Spectroscopy, 5 (2003) 6.
37 J. E. Davies and N. Baldan, J. Biomed. Mater. Res., 36 (1997) 429.
38 M. M. Hosseini, J. Sodek, R. P. Franke and J. E. Davies, The structure and composition of the bone implant interface. In: J. E. Davies (Ed.) Bone engineering, Toronto, Em squared Inc 2000, p. 295.
39 E. D. Eanes, Dynamics of calcium phosphate precipitation. In: E. Bonucci (Ed.), 'Calcification in Biological Systems', Boca Raton, CRC Press 1992, p. 1.
40 H. M. Kim, F. Miyaji, T. Kokubo and T. Nakamura, J. Biomed. Mat. Res., 32 (1996) 409.
41 M. C. de Andrade, M. R. T. Filgueiras and T. Ogasawara, J. Biomed. Mat. Res., 46 (1999) 441.
42 S. Kačiulis, G. Mattogno, L. Pandolfi, M. Cavalli, G. Gnappi and A. Montenero, Appl. Surf. Sci., 151 (1999) 1.
43 H. Takadama, H. M. Kim, T. Kokubo and T. Nakamura, J. Biomed. Mater. Res., 55 (2001) 185.
44 J. Šesták, J. Therm. Anal. Cal., 61 (2000) 305.
45 N. Koga, Z. Strnad, J. Šesták and J. Strnad, J. Therm. Anal. Cal., 71 (2003) 927.